SST and wind stress perturbations for seasonal and annual simulations

Seasonal Forecast Section, ECMWF
Antje.Weisheimer@ecmwf.int

12 December 2005

Dynamical ensemble seasonal forecasting requires a set of different, but consistent initial conditions for the atmosphere and ocean components of the coupled model. Simulations are carried out starting with each of these initial conditions leading to an ensemble of forecasts. The initial conditions are consistent in the sense that they are designed to represent the inherent uncertainties in the operational analyses. A set of initial conditions is created by adding small perturbations to an initial best-guess unperturbed state. For the atmosphere, these perturbations are calculated using the singular vector method, which computes the modes of the fastest energy growth during the first two days of the forecasts. The ensemble of initial conditions for ocean model forecasts is created by adding small perturbations to the sea surface temperatures (SST). Furthermore, the wind stress field is perturbed every day. This documentation describes how the SST and wind stress perturbations are estimated in the operational seasonal forecasts. For the simulations carried out in the ENSEMBLES project the same strategy is used.

1. SST perturbations

Several data sets of SST analyses are available. They have been generated based on different analysis schemes, using various observational data and also differ in their lengths and averaging periods. The differences between these SST analysis data sets are supposed to reflect the inherent uncertainty in the SST analysis.

Global sets of SST products are generated as monthly or weekly means, whereas the ocean model requires the forcing fields on a daily basis. Thus the SSTs are interpolated to daily values. A quantitative estimate of the interpolation effect can be obtained by comparing results from monthly/weekly interpolation with a different daily data set (NCEP) used in the operational medium-range forecasts. Therefore, the SST perturbations applied in the ensemble seasonal forecasts are based on uncertainty estimates due to differences in different SST analyses as well as due to interpolation effects.

In the following we distinguish two distinct time periods, before and after the 1980s, because different SST analyses data sets are available for these periods. The main difference is the availability of satellite-derived products starting in the 1980s. Therefore, two separate strategies have been considered to create the sets of SST perturbations for each period.

1.1 SST perturbations after 1980s

For the 20-year period from 1982 to 2001 a set of SST perturbations has been constructed by taking the differences between the Reynolds 2DVAR (based on a 2-dimensional variational assimilation scheme) and Reynolds OIv2 (based on an optimal interpolation scheme) SST analysis products. Both products are provided as weekly mean fields. The procedure of generating the perturbations involves interpolating daily values and computing the 20-year climatology for both products. The SST perturbations are capped if they exceed a certain threshold value XCAP. The recommended value is for SST perturbations after 1980 is XCAP=1.0. In order to have a 3 dimensional structure in the ocean, the SST perturbations are linearly interpolated to a depth of 40m.

The following plots show examples of perturbation (fig.1) due to uncertainties in the different ocean analysis data sets on a weekly-mean basis and due to uncertainties in the interpolation from weekly averages to daily data (fig. 3) together with the corresponding annual standard deviations (fig. 2 and 4). The sensitivity of the perturbation's standard deviation to the capping threshold value is shown in Fig. 5. The perturbations based on uncertainties in the two ocean analyses are largest in the Southern Ocean, in parts of the Pacific and in the North Atlantic, whereas perturbation in the Indian Ocean are also large due to the time interpolation discussed above. Highest variances occur in the North Atlantic, the Arctic and Southern Oceans.

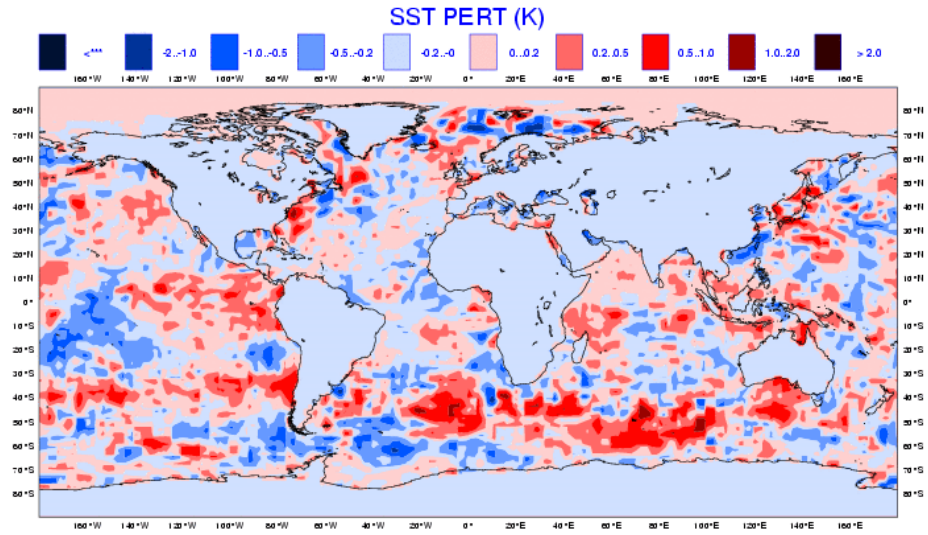

Fig.1 : Random example of the SST perturbations based on uncertainties in the ocean analysis (Reynolds 2DVAR and Reynolds OIv2) for the period after 1980.

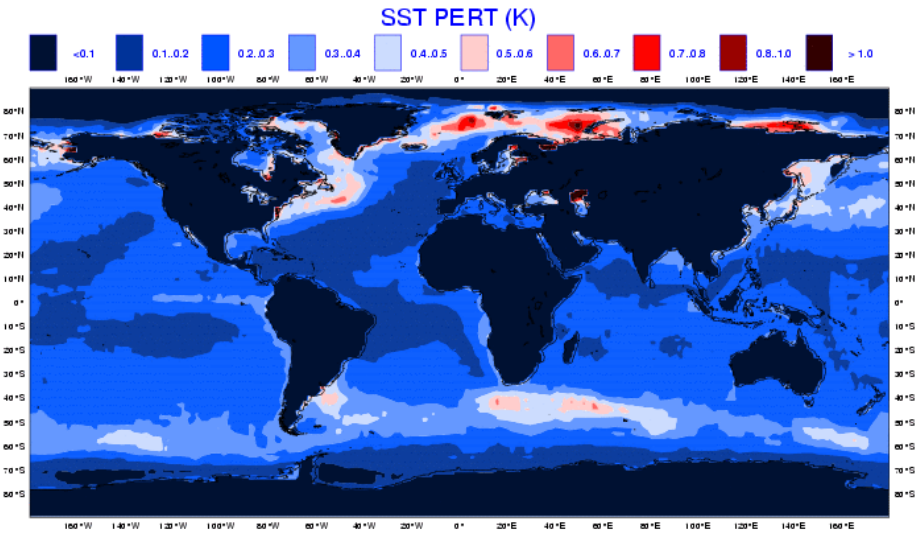

Fig. 2: Standard deviation of the SST perturbations based on uncertainties in the ocean analysis (Reynolds 2DVAR and Reynolds OIv2) for the period after 1980.

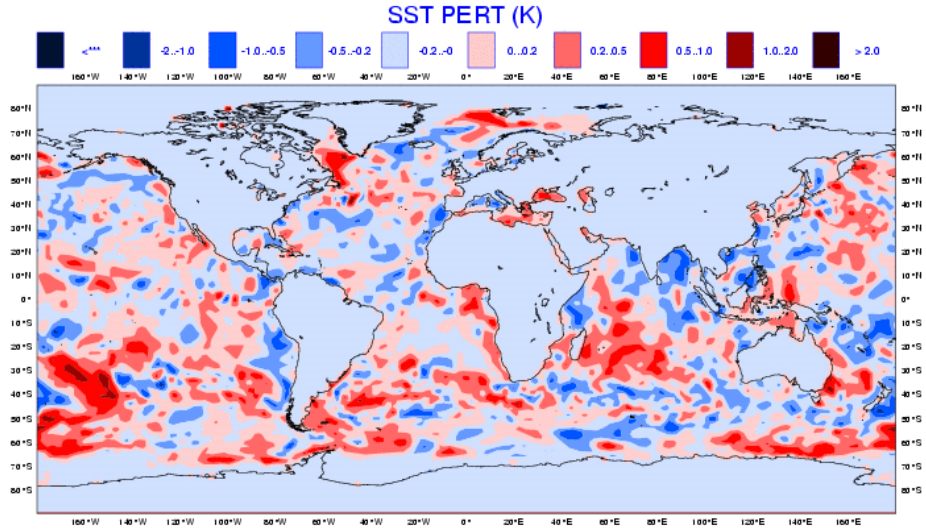

Fig. 3: Random example of the SST perturbations based on uncertainties due to the interpolation of weekly averages to daily data for the period after 1980.

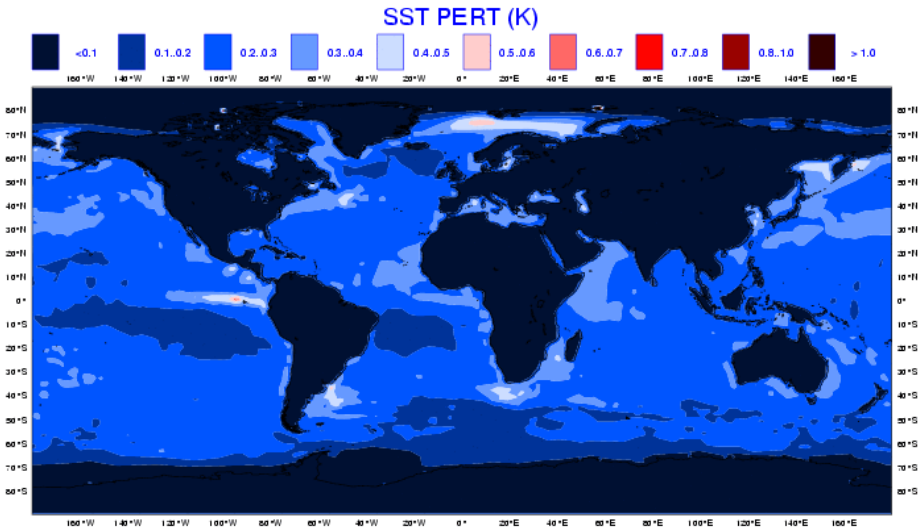

Fig. 4: Standard deviation of the SST perturbations based on uncertainties due to the interpolation of weekly averages to daily data for the period after 1980.

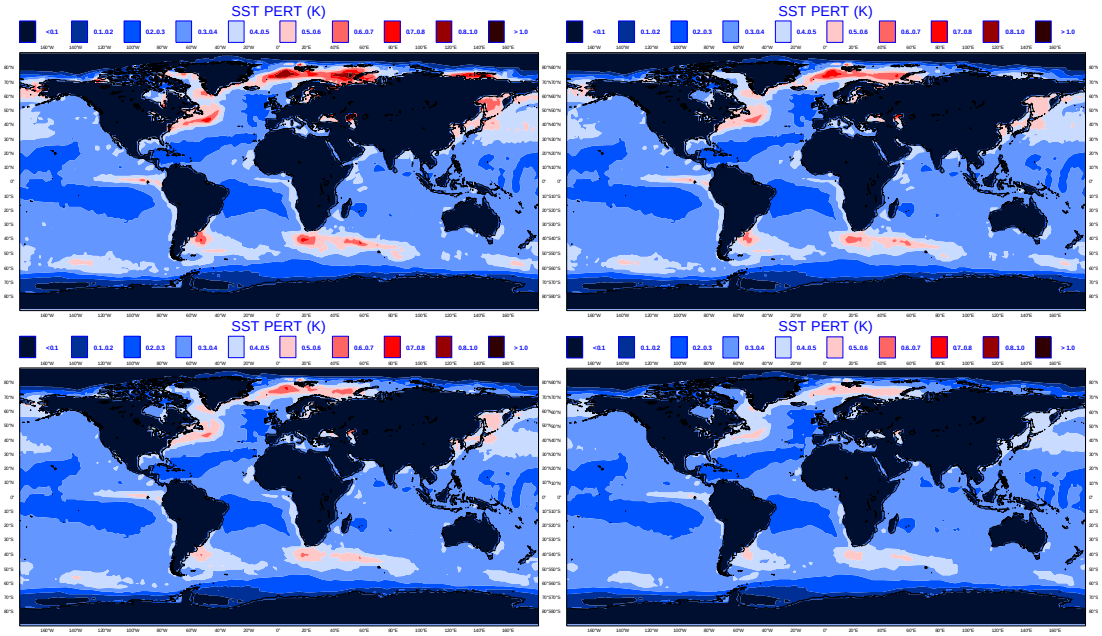

Fig. 5: Impact of the caping of the SST perturbations on the standard deviation. top left) no capping; top right) XCAP=1.2; bottom left) XCAP=1.0; bottom right) XCAP=0.8.

1.2 SST perturbations before 1980s

Before 1980s, that is for the 30-year period from 1951-1980, time interpolated differences between the NCEP ERSSTv2 and Hadley SSTs (HadISST1.1) products have been used to generate the perturbations. Both SST products are based on monthly mean SSTs (instead of weekly means after 1980) and use SST EOF reconstruction. ERSSTv2 has a 2x2 resolution; HadISST1.1 a 1x1 resolution. The recommended capping threshold before 1980 is XCAP=1.4. Figures 6-9 show similar plots as Fig. 1-4, but for the period before 1980. Due to the sparse coverage of the global ocean with observational data in the pre-satellite period, the uncertainties in the SST analyses are larger than those after 1980. This leads directly to an increase in magnitude of the perturbations themselves as well as to larger standard deviations.

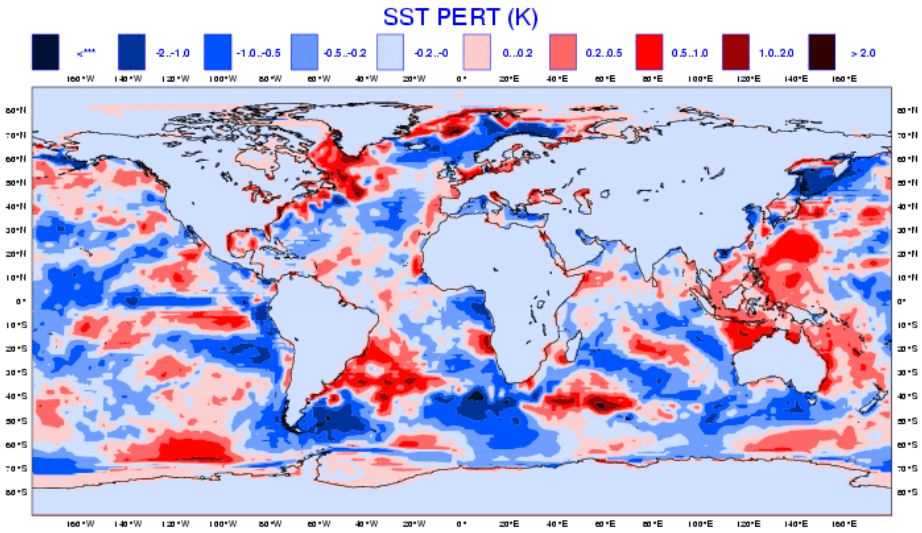

Fig.6 : Random example of the SST perturbations based on uncertainties in the ocean analysis (NCEP ERSSTv2 and Hadley SST) for the period before 1980.

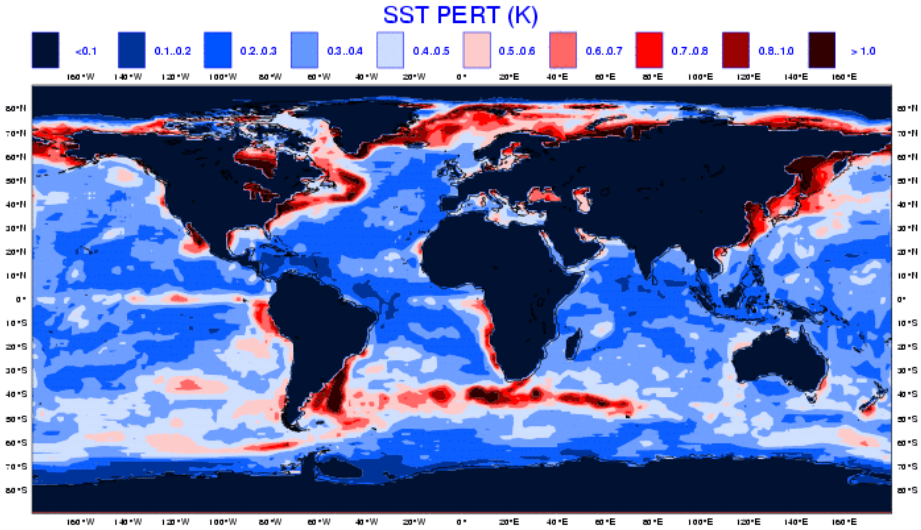

Fig. 7: Standard deviation of the SST perturbations based on uncertainties in the ocean analysis (NCEP ERSSTv2 and Hadley SST) before 1980.

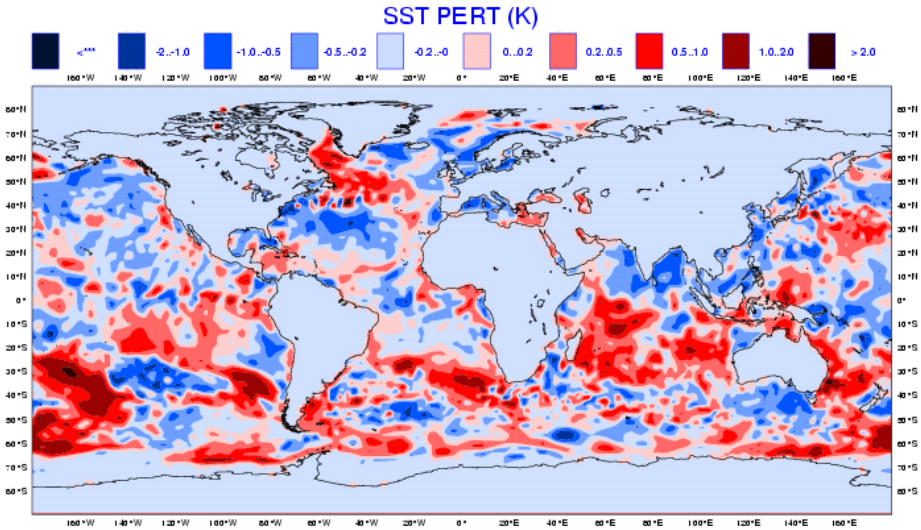

Fig. 8: Random example of the SST perturbations based on uncertainties due to the interpolation of monthly averages to daily data for the period before 1980.

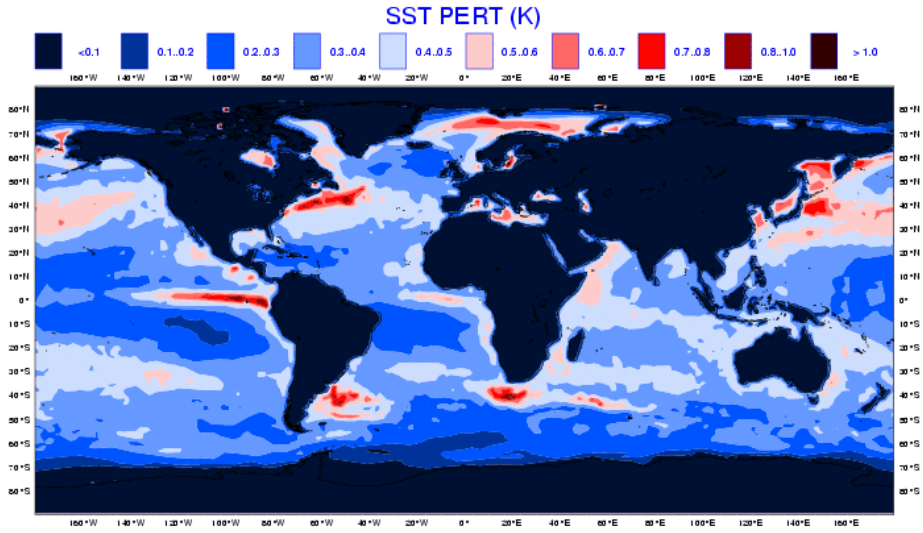

Fig. 9: Standard deviation of the SST perturbations based on uncertainties due to the interpolation of monthly averages to daily data for the period before 1980.

2. Wind stress perturbations

Following the same concept discussed for the SST above, wind stress perturbations are calculated from the differences between different wind stress data sets. In the new operational seasonal forecast system at ECMWF (system 3) the wind stress perturbations are computed as differences between the CORE and ERA40 data sets. For the ENSEMBLES simulations we also use these new wind stress perturbations. For the sake of comparison, we show the old set of perturbations used in system 2, which were based on differences between ERA15 and SOC wind stress data. This set of old perturbations was used for the DEMETER runs. Documentations about the way the old perturbations had been computed can be found at:
http://www.ecmwf.int/research/monthly_forecasting/pert.html
and http://www.ecmwf.int/research/demeter/news/info/modelling.html

2.1 Data sets

Four different data sets have been considered to compute the wind perturbations required to generate the seasonal forecast ensembles:

- ERA40, available from 1958 to 2001
- ERA15, available from 1979 to 1993
- CORE, available from 1958 to 2000
- SOC, available from 1980 to 1997

The ERA40 files are stored in ec:/ocx/forcing/e4/, one file per month, on a 256x128 Gaussian grid from North to South. The files contain daily values of analysis and forecast data. The forecast data have been computed as accumulated fluxes over the initial 24 hours of the ERA40 forecasts.

ERA15 covered the period 1979-1993. They are in ec:/ocx/forcing/er in similar format as ERA40.

The CORE data were obtained from http://data1.gfdl.noaa.gov/nomads/froms/mom4/CORE.html where a detailed technical documentation is available. Here the wind stress is computed from 6-hourly analysis data. The data are written in a 192x94 regular grid (T85) in GRIB and NetCDF format. and stored in ec:/nep/datos/core, one file per year.

The SOC data came from the Southampton Oceanography Centre and was a global monthly analysis of wind stress on a 1x1 degree grid. In contrast to the other data sets, the SOC analysis is solely based on surface observations and does not use satellite data.

Three different sets of perturbations have then been created: the differences between monthly mean CORE and SOC anomalies with the corresponding ERA40 anomalies as reference, and between monthly mean SOC anomalies with the corresponding ERA15 reference anomalies. Due to the large impact of remote sensing data products on the wind stress analyses, a distinction has been made between the pre-satellite and satellite era. Results for the following periods and data sets will be shown and discussed in the course of the text:

- 1958-2000: ERA40-CORE full period
- 1958-1979: ERA40-CORE pre-satellite period
- 1980-2000: ERA40-CORE satellite period
- 1986-1993: ERA15-SOC
- 1980-1997: ERA40-SOC

2.2 System 3 perturbations

Figures 10 and 11 show the median and standard deviation for the January zonal and meridional wind stress perturbations τ_x and τ_y based on differences between ERA40 and CORE for the full period from 1958 to 2000. A general feature of the perturbations is that, because of looking at differences between anomalies, the mean of the differences should always be close to zero. The standard deviation is largest in the equatorial Pacific and in the Southern Hemisphere, The wind perturbations are skewed, as the mean and the median are different; however, the skewness is not too large, as the 5% and 95% percentiles are close to mirror images (not shown).

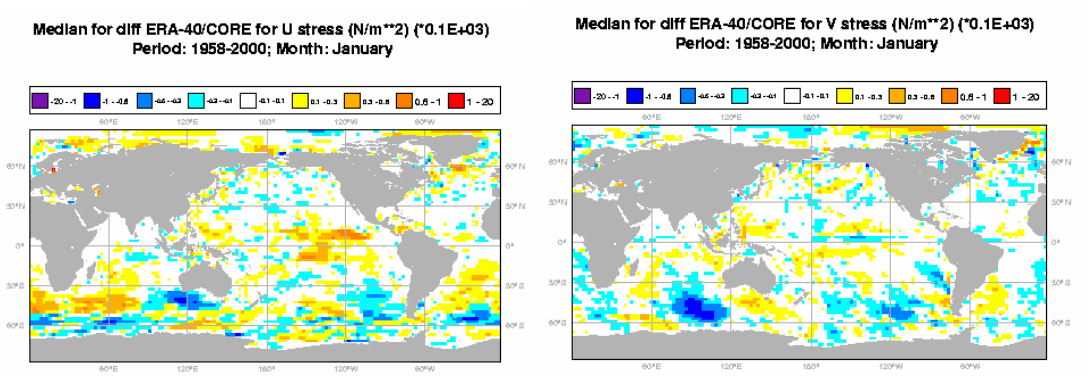

Fig. 10: Median of the wind stress perturbations (left: zonal component τ_x; right: meridional component τ_y) based on differences between ERA40 and CORE for the January months of 1958-2000.

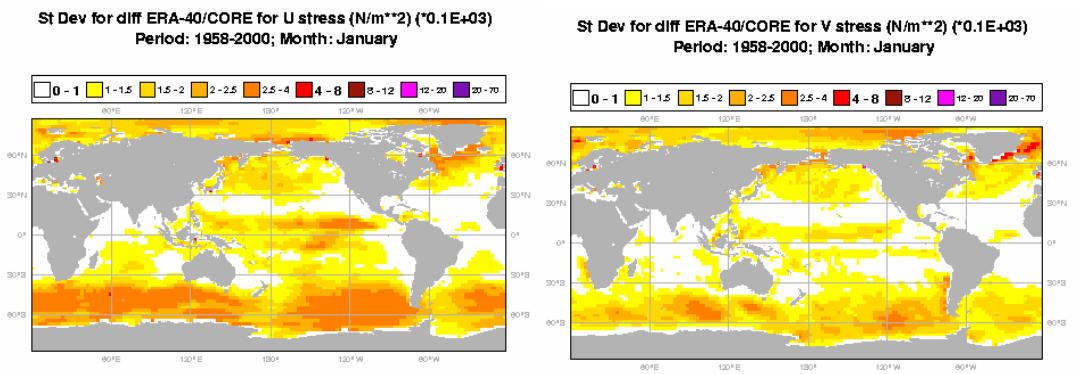

Fig. 11: Standard deviation of the wind stress perturbations (left: zonal component τ_x; right: meridional component τ_y) based on differences between ERA40 and CORE for the January months of 1958-2000.

Figures 12 and 13 show the January zonal wind stress median and standard deviation for both, the pre-satellite period from 1958-1979 and the satellite period 1980-2000 for ERA40-CORE differences. The introduction of satellite products has clearly reduced the uncertainties between the two different data sets: the median and standard deviations of the perturbations decreased, especially over the otherwise sparsely data covered Southern Oceans. The skewness of the differences has also changed, suggesting slight changes in the PDFs of each wind stress data set.

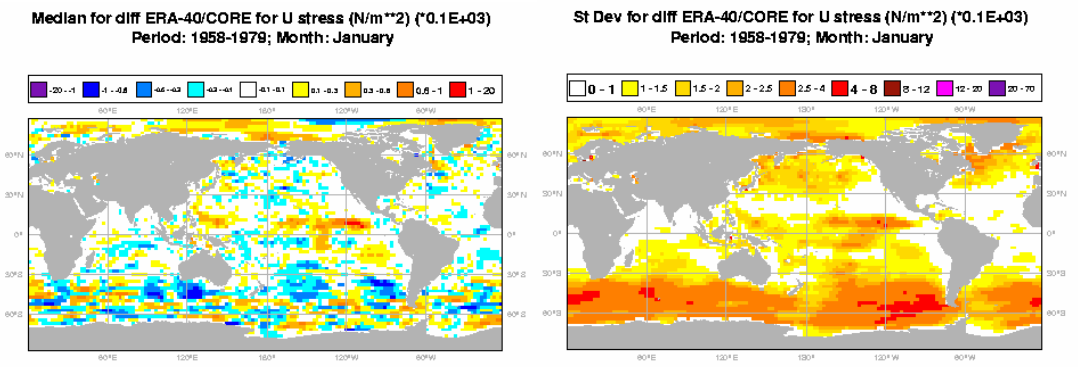

Fig. 12: Median (left) and standard deviation (right) of the zonal wind stress perturbations based on differences between ERA40 and CORE for the January months of the pre-satellite period 1958-1979.

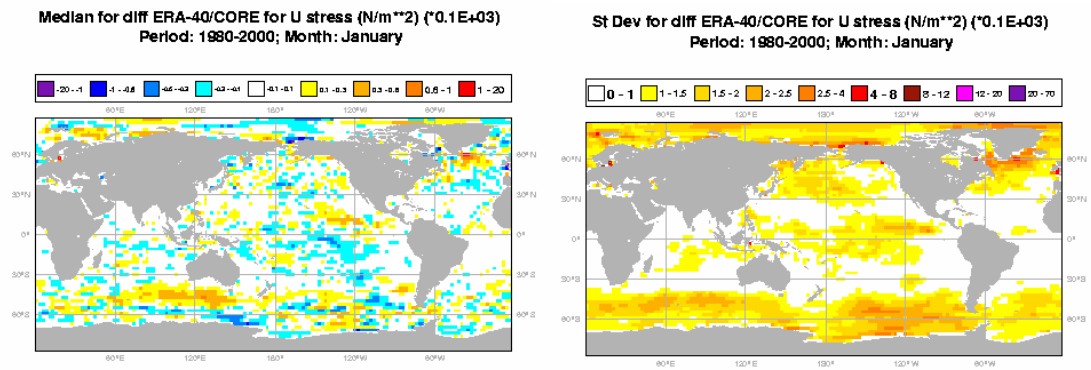

Fig. 13: Median (left) and standard deviation (right) of the zonal wind stress perturbations based on differences between ERA40 and CORE for the January months of the satellite period 1980-2000.

Similar comparisons have been made for July. The main findings are larger perturbations, in terms of median and standard deviation, over the Southern Hemisphere Ocean and a reduction in amplitude and standard deviation over the Northern Hemisphere (fig. 14). The intra-annual variability in the strength of the differences is most pronounced in the pre-satellite period (not shown) and appears with a similar spatial structure but weaker amplitude after the 1980s.

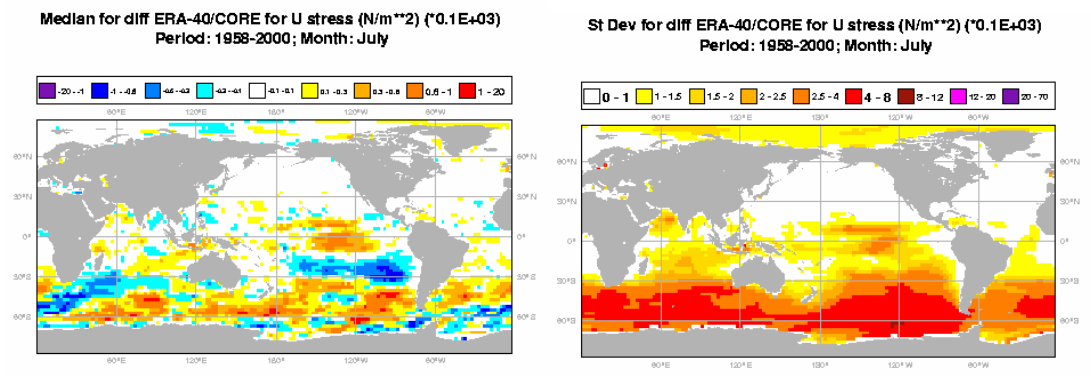

Fig. 14: Median (left) and standard deviation (right) of the zonal wind stress perturbations based on differences between ERA40 and CORE for the July months of the period 1958-2000.

2.3 System 2 perturbations

For the sake of comparison, figure 15 shows the old perturbations as used in system 2 (and DEMETER). Those were based on differences between ERA15 and SOC for the period 1986-1993.

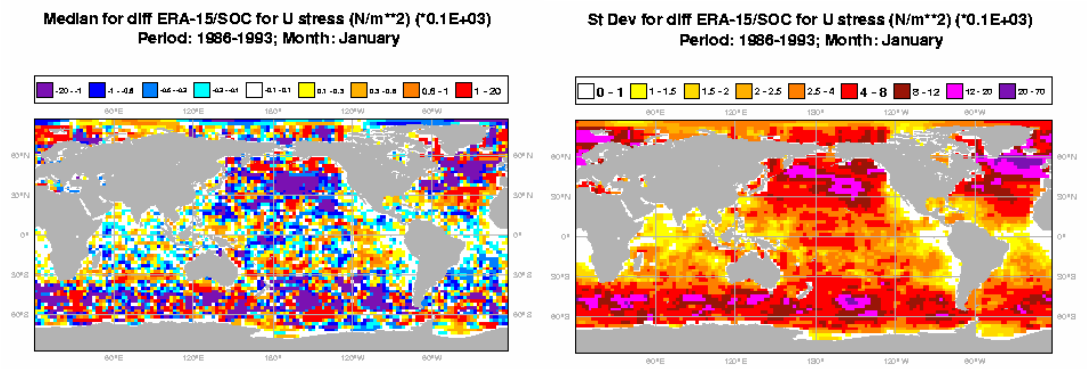

Fig. 15: Median (left) and standard deviation (right) of the zonal wind stress perturbations based on differences between ERA15 and SOC for the January months of the period 1986-1993.

The “old” system 2 ERA15-SOC perturbations have a much larger (more than double) amplitude than the “new” system 3 ERA40-CORE perturbations (cf Fig. 13, note the similar colour scale). This means that the ERA40 and CORE climatologies bear stronger similarities than ERA15 and SOC, especially over the Southern Hemisphere where there were very few observational data available. The larger perturbations in system 2 are partly due to the fact that SOC does not include satellite data.

The reference data for the “old” system 2 perturbations in figure 15 were ERA15. However, the reference data for the “new” system 3 perturbations are the latest European re-analyses ERA40 (fig. 13). In order to estimate the impact of a different data set, i.e. CORE analysis vs. SOC data, while having the same reference ERA data, differences between ERA40 and SOC are plotted in figure 16. Note the slightly different time period. The results are very similar to those using ERA15, suggesting that the main reason of having reduced perturbations in system 3 is indeed the CORE data set, rather than the reference re-analysis used.

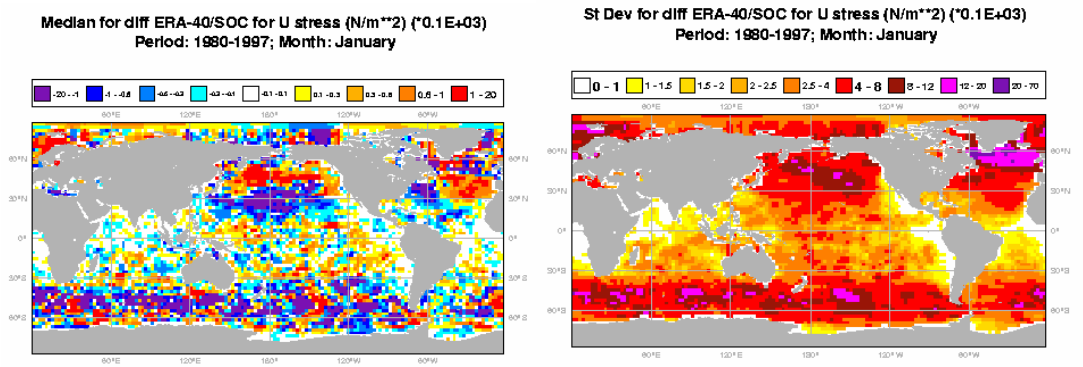

Fig. 16: Median (left) and standard deviation (right) of the zonal wind stress perturbations based on differences between ERA40 and SOC for the January months of the period 1980-1997.